Materials Science Forum
ISSN: 1662-9752, Vol. 1133, pp 55-66
doi:10.4028/p-5bbeeB

Submitted: 2024-08-23
Accepted: 2024-08-27
Online: 2024-12-10

Target Alloys of Iron-Based Materials through CALPHAD Method

Yusuf Faqiri[1,a*] and Thomas Hassel[1,b]

[1]Institut für Werkstoffkunde (Materials Science), Leibniz University Hanover, 30823 Garbsen, Germany

[a*]faqiri@iw.uni-hannover.de, [b]hassel@iw.uni-hannover.de

Keywords: Computer aided modelling, CALPHAD, Plasma Transferred Arc Welding, Alloys, JMatPro

Abstract. The development of tailored alloys is an important aspect for enhancing efficiency across diverse applications in mechanical engineering. The use of computer-aided modelling offers an opportunity to enable a more efficient and targeted material development. In the present work, new iron-based alloys with specific properties were developed using the CALPHAD method. The alloy design developing process was carried out by using the simulation software JMatPro® and the data evaluation software EDA®. Using a full factorial plan, various alloys were modelled on the basis of the elements iron, nickel, vanadium, carbon, niobium and chromium. Afterwards, the alloys were narrowed down with regard to the criteria of carbide phase content, formability, and corrosion resistance. Subsequently, two final alloys were chosen based on their properties. Afterwards the selected final alloys were produced by mechanically blending different powder alloys and elements. These alloys were welded onto unalloyed steel using Plasma Transferred Arc welding and were characterised by using x-ray diffraction, scanning electron microscopy, hardness measurements, spark spectrometry and metallography. Subsequently, a verification of the welded samples regarding to chemical composition, phases, and corrosion resistance was carried out. The investigations showed that it was possible to simulate alloys with specific properties using computer-based software, which corresponded with the experimental studies.

Introduction

Steel is still the most commonly used alloy in industry due to its superior mechanical properties and versatility. The respective application is always connected to the corresponding requirements in terms of mechanical and chemical properties. These properties are in turn influenced by the chemical composition and microstructure of the steel. Furthermore, the involved elements interact with each other in a temperature dependent manner, resulting in complex interactions between the alloying elements. Due to the numerous possible combinations of the individual alloying elements, there exists an almost unlimited variety of alloying possibilities. Accordingly, the alloy development of new steels is a complex process. In the past, the development of new alloys was mainly based on the empirical correlation of chemical composition and the resulting properties. This involves testing and analysing various combinations and ratios of alloying elements. Accordingly, the time and costs involved are very high, especially when more than ternary material systems are being analysed. Therefore, new methods are required that have a resource-efficient and economic advantage over empirical materials development. In this regard, the use of computer-aided modelling presents an opportunity to enable a more efficient and targeted materials development. Modern material simulation programs such as JMatPro® or ThermoCalc® calculate phase diagrams of alloys based on their chemical composition. The calculation approach is based on the CALPHAD method (CALculation of PHAse Diagrams) [1]. In combination with a Materials Data System, such as EDA®, targeted material modelling can be carried out. Chen et al. [2] investigated the material behaviour and heat treatment process parameters of high-molybdenum-vanadium high-speed steel using JMatPro®. The objective was to increase the content of molybdenum and vanadium while simultaneously reducing the tungsten content. Therefore, they used JMatPro® for analysing the phase composition at various temperatures according to the content of the elements. They optimized the

carbon content of the alloys and also the process parameters of heat treatment, which included the quenching, annealing, and tempering temperatures. Zhang et al. [3] focused their work on a dilatometric study of high alloy martensitic tool steel produced through the powder metallurgy process. The objective was to create a Continuous Cooling Transformation (CCT) diagram for the investigated steel at various cooling rates, involving a comparison of surface hardness across different samples with specified cooling rates. JMatPro® software was employed to compare experimentally measured CCT diagrams with simulated values. It was demonstrated that the software proved to be a valuable tool for a rough estimation of the CCT, however, achieving full correlation with the experimental data was not possible. Further Dykas et al. [4] focused on modelling phase diagrams and CCT diagrams of medium manganese steels. Therefore, they used computational tools such as ThermoCalc® and JMatPro® to simulate phase transformations under varying temperature and time conditions. The aim was to analyse the influence of alloying elements manganese (Mn) and carbon (C), on the stability of phases during heat treatments. The results of the computational and modelling analyses were used to demonstrate the effect of alloying elements on both equilibrium and non-equilibrium phase diagrams, as well as on the evolution of microstructure and chemical composition. Cha et al. [5] utilized CALPHAD-based computational techniques to develop advanced carburizing steels for automotive applications. Therefore, they designed a new alloy system for advanced bearing steels to enhance the strength, hardenability, and hardness with optimized cementite size distribution. The strength of the modified bearing steel was enhanced by the addition of 0.2 wt% vanadium through the formation of fine vanadium carbide precipitates. Experimental validation of the calculated results affirmed the reliability of the computational method.

Aim of the Work

The aim of this work was to develop new iron-based alloys for the Collaborative Research Centre 1153 (CRC 1153) “Tailored Forming” by computer aided modelling. Tailored Forming is a new process chain for the manufacturing of hybrid components with locally adapted properties. The process chain is divided into three sections, as shown in Fig. 1. In the first section, the manufacturing of the hybrid semi-finished product is carried out by using a joining process, such as deposition welding. Afterwards, the component is formed by means of a forging process. In the last section the component is heat treated and machined. The result is a hybrid component that is subjected to an appropriate lifetime test.

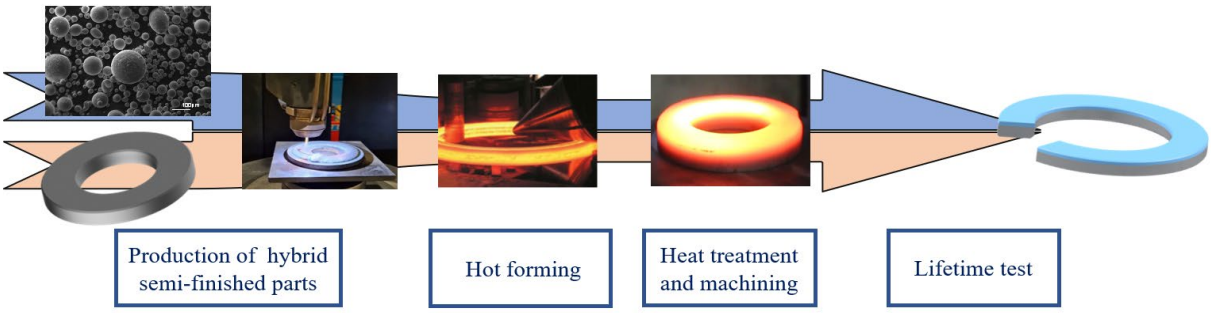

Fig. 1. Tailored Forming process chain

The process chain shows that the alloys must have certain properties in order to be used. The locally adapted properties of the tailored forming components are designed in such a way that the highly stressed areas have to withstand high tribological loads. Therefore, a necessary requirement is that the alloy is characterized by a high hardness and wear resistance. Due to the existing forging process, a second essential requirement for the alloy is a corresponding formability. Furthermore, the components are used in a corrosive environment, which is why a corrosion-resistant alloy is required. In previous studies, the commercial bearing steel 100Cr6 was used due to its wear resistance, hardness, and fatigue resistance [6]. Because of the limited corrosion resistance of 100Cr6, a new alloy was developed in a subsequent investigation, which exhibited both corrosion and wear

resistance [7]. The development process was conducted empirically by testing various alloy compositions. Further investigations revealed that this newly developed alloy demonstrated more consistent fatigue properties than 100Cr6. Moreover, in the tribological service life test FE8 according to DIN 51819 [8], the new developed alloy outperformed 100Cr6 by lasting longer. However, the alloy showed insufficient forming properties while exhibiting good wear resistance. Accordingly, further alloys that are suitable for the tailored forming process need to be systematically investigated. Therefore, the goal of this paper was to develop new iron-based alloys that are simultaneously wear resistant, forgeable and corrosion resistant. For this purpose, a computer-aided material development was carried out using JMatPro® and EDA®. The final selected alloys were produced using Plasma-Transferred-Arc (PTA) welding.

Material and Methods

Computer aided alloy design

The process of alloy development is illustrated in Fig. 2. The red marked box represents the computer aided alloy design part.

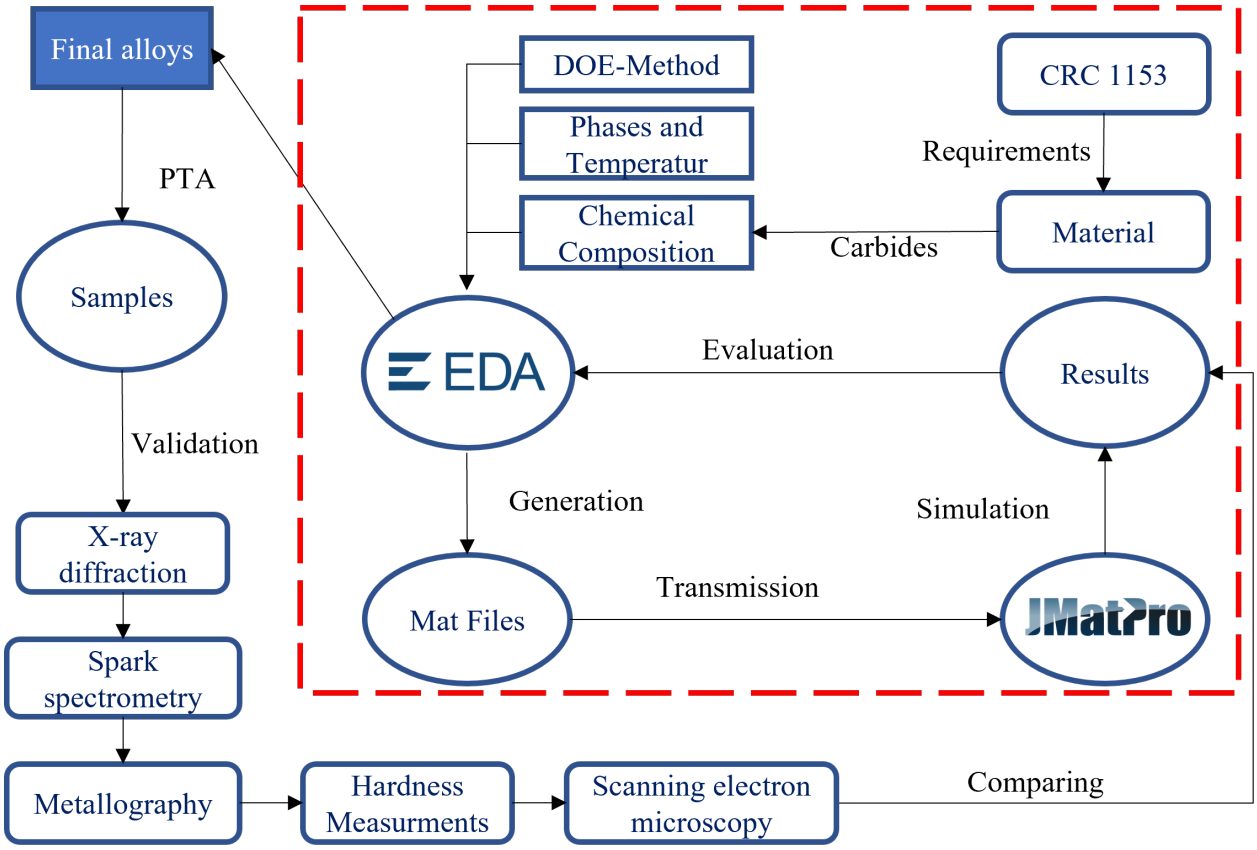

Fig. 2. Computer aided modelling schema for new Tailored Forming alloys

First, the chemical composition of the alloys was defined in EDA®. For this purpose, specific elements were selected with consideration of the target properties regarding formability, corrosion resistance, and hardness. To ensure hardness, the elements carbon (C), vanadium (V), and niobium (Nb) were selected. Carbon has a strong influence on the material properties and influence the formation and precipitation of carbides in alloys [9]. Niobium and vanadium react preferentially with carbon and lead to the formation of carbides, which increase the wear resistance and hardness [10]. To enhance wear and corrosion resistance the element chromium (Cr) was chosen [11]. The element nickel (Ni) was also considered, as it is a strong austenite former and effects positive the forming behaviour [12]. Trace elements such as nitrogen (N) and oxygen (O) were also taken into account. Furthermore, it was necessary to define the considered phases and temperatures for the calculations. All-important phases influenced by the mentioned elements have been selected, above all, carbide

types such as MC, M_2C, $M_{23}C6$ and M_7C_3. The temperature range was defined from 1600°C to 600°C, with calculation steps of 10°C. In the final step, a full factorial design in EDA was selected for the DOE method, ensuring that all possible combinations of the individual elements are considered. For this purpose, a minimum and maximum weight percent of each alloying element was determined, as well as an appropriate calculation step size. The weight percent intervals of the elements and their respective calculation steps are showed in Table 1. The carbon content ranges from 0.5 to 1 wt%. The chromium content is maintained from 12 - 22 wt% to ensure corrosion resistance. A mass content interval of 1-11 wt% was considered for nickel, niobium and vanadium. The calculation step size for adjusting each element is 1 wt%, except for carbon, where it is 0.1 wt%.

Table 1. Composition range

Element	Fe	Cr	C	Ni	Nb	V
Wt% min.	Bal.	12.0	0.5	1.0	1.0	1.0
Wt% max.	-	22.0	1.0	11.0	11.0	11.0
Calculation step	-	1.0	0.1	1.0	1.0	1.0

After defining the required information, EDA® generates corresponding MAT-FILES for each simulated alloy. The alloys result from the full factorial plan, which considers the alloying elements, their weight percent intervals, and calculation step size. The MAT-FILES were then transferred to JMatPro®, where corresponding equilibrium calculations were performed using the CALPHAD method, taking the previously defined phases, temperature range and calculation steps into account. Afterwards, the evaluation of the calculations was carried out in EDA®, where all simulated alloys were analysed according to the specified requirements.

Manufacturing Process and Material Analysis

Plasma-Transferred-Arc welding was used to produce the selected final alloys. The PTA process is a thermal coating process used for the wear protection of highly stressed components [13]. During the welding process, a high-density plasma arc is created using a tungsten cathode, reaching temperatures between 10,000°C and 15,000°C. This arc melts the surface of the base material and simultaneously, cladding powder is fed into the arc, melting and establishing a substance-to-substance bond between the cladding and the base material [14]. As fed, plasma and shielding gas argon is used. The advantages of the PTA process are a high degree of automation and low dilution between the base and cladding material. A further benefit is that the filler material is in powder form [15]. Therefore, in the presence of two or more powder feeders, it is possible to mix different alloys in-situ and thus produce new alloys. To produce the predicted alloys, industrially available alloy powders and single elements powders were mixed together in different ratios. The mixing was performed manually for a duration of 5 minutes for each alloy. The grain size of all powders was between 63 µm and 200 µm, according to the current industrial standard for additional materials for PTA welding [16]. The used powders, as well as the manufacturers and chemical composition, are specified in Table 2.

Table 2. Chemical composition of the cladding and base material in wt%

Alloy name	Manufacturer	C	Cr	Nb	Ni	V	Fe
FeNb	Nt-Systemlösungen GmbH	0.12	-	66.4	-	-	Bal.
Rockit 706	Höganäs AB	2.60	4.9	-	-	6.1	Bal.
Rockit 401	Höganäs AB	-	18.3		2.5		Bal.
NiCr8020	Nt-Systemlösungen GmbH	0.10	20.0	-	Bal.	-	-
316L	Nt-Systemlösungen GmbH	0.03	17.0	-	12.0	-	Bal.
Ni-Powder	Corodur GmbH	0.10	-	-	Bal.	-	-
C-Powder	Corodur GmbH	Bal.	-	-	-	-	-

The welding process was carried out by a six-axis Kuka industrial robot (KUKA AG, Augsburg, Germany), with two additional axes realised by a tilt and turn table. The welding torch was a water cooled PTR450 (Autogen-Ritter GmbH, Munich, Germany) applied on the current source PSI 400 (Kjellberg Finsterwalde GmbH, Finsterwalde, Germany). The current source has a maximum output of 400 A and can achieve feed rates of up to 20 kg/h. The alloys were welded on unalloyed steel plates made of S355. The welding current utilized was 140 A, with a plasma gas flow rate of 1.5 l/min. Argon was used as shielding, plasma and feeding gas.

Material Analysis

In order to evaluate the microstructure of the welded alloys, metallographic examinations, spark spectrometry, hardness measurements, X-ray diffraction (XRD) and Energy-dispersive X-ray spectroscopy (EDX) were carried out after welding. By utilizing optical light microscopy, the observation and characterization of different phases in the microstructure are enabled. This allows for a detailed analysis of the various sizes and shapes of micron-sized carbides. The images of the microstructure were captured using the ZEISS OLYMPUS BX53M microscope (Olympus Corporation, Shinjuku, Japan). For the metallographic preparation, the samples were polished and etched with 2% Nital (nitric acid and ethanol). Spark spectrometry was used to determine the elemental composition of the welded alloys. This ensures that the elemental composition of the alloys is within the specified limits, which is important for maintaining the required material properties. The corresponding measurements was carried out with the “SPECTROMAXx” spark spectrometer (Spectro Analytical Instruments GmbH, Kleve, Germany). Vickers hardness measurements were performed by Qness 60 (ATM Qness GmbH, Mammelzen, Germany) micro hardness tester. XRD methodology enables a qualitative analysis of phases. Due to the distinct peaks of the carbides, they can be determined precisely. Accordingly, this measurement technique was employed to detect the expected phases in the welded samples. The phases and carbides were determined by using the BRUKER D8 (Bruker Corporation, Massachusetts, USA) with the aid of Co-Kα radiation. EDX is able to analyse the concentration of elements within material micro regions by using the different quantum energies of the emitted X-rays. It is possible to take measurements at individual points, along lines or over entire areas, creating distribution images that show the content of the individual elements. EDX linescans and mappings of the welded alloys were carried out with the Supra 40VP SEM (Carl Zeis, Oberkochen, Germany).

Results and Discussion

Simulation Results. Based on the alloying elements, their weight percent intervals, and calculation step size, EDA® generated more than 87,846 possible alloys within the full factorial experimental design. Afterwards, the alloys were calculated in JMatPro® and subsequently evaluated in EDA® based on the criteria of corrosion resistance, formability, and hardness, as shown in Fig. 3. It is essential to ensure that the minimum amount of iron (Fe) was at least 75 wt%, in accordance with the iron calculation model of JMatPro®. Accordingly, all alloy with less than 75 wt% Fe was removed, resulting in 3630 alloys. Due to the high chemical affinity of chromium for carbon, Cr23C6 precipitations occur at the grain boundaries. To ensure corrosion resistance, 12 wt% of free dissolved chromium in the matrix is required to form a passivation layer. If this con-tent is lower due to the formation of chromium carbides, corrosion resistance is no longer guaranteed and lead to intergranular corrosion at grain boundaries or areas adjacent to them.

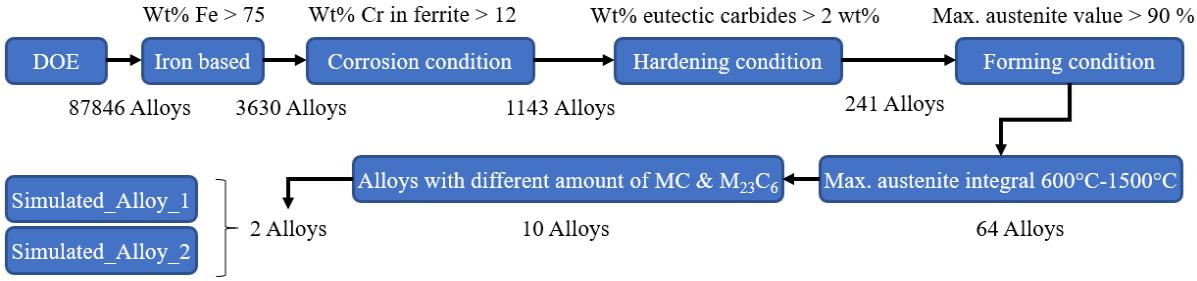

Fig. 3. Schematic procedure for the delimitation of alloys

Therefore, a necessary condition for corrosion resistance is that at least 12 wt% of chromium is bound in the matrix phase. In the first step, using EDA®, the free dis-solved chromium content of the ferritic matrix was examined at 600 °C. All alloys that did not meet the criterion for corrosion resistance were filtered out, resulting in 1143 remaining alloys. In addition to carbides precipitated directly from liquid melt, eutectic carbides are also required to achieve hardenability. Unlike the carbides mentioned before, the eutectic carbides dissolve during austenitisation and contribute to secondary hardening [17]. Accordingly, a minimum content of 2 wt% eutectic car-bides was assumed for the remaining alloys. The criteria mentioned above were fulfilled by a total of 241 alloys. The next step was to filter out all alloys with a maxi-mum austenite value of less than 90%, as austenite favours the formability of mate-rials. This resulted in the elimination of a further 177 alloys. However, the maximum austenite value does not provide information about the austenite temperature interval through which it extends. A higher austenite interval generally has a more favour-able impact on the formability properties because deformation never occurs adiabatically, and the material temperature decreases during formation. To identify alloys with the highest austenite phase fraction for the temperature range between 600°C and 1500°C, the respective integrals of the remaining alloys were calculated. The 10 alloys with the highest integral values were selected and examined regarding their MC and M23C6 carbide contents. Subsequently, 2 alloys were selected, which have different proportions of these carbides, as shown in Fig. 5. The alloys were named “Simulated_Alloy_1“[SA1] and “Simulated_Alloy_2” [SA2]. The alloys differ in their C, Cr, and Nb contents. SA1 has a carbon content of 0.7 wt%, a chromium content of 14 wt%, and a Nb content of 4 wt%. In contrast, SA2 has a lower carbon content of 0.5 wt%, a chromium content of 15 wt%, and a Nb content of 2 wt%. Since Nb promotes the formation of MC carbides, SA1 has significantly higher MC carbide content compared to SA2, but less $M_{23}C_6$ carbides. The amount of Ni and V are in both alloys the same. The chemical composition and carbide contents of the alloys is shown in Table 3.

Table 3. Composition and carbide content of the selected alloys in wt%.

Name	Fe	C	Cr	Nb	Ni	V	MC	$M_{23}C_6$
Simulated_Alloy_1	Bal.	0.7	14.0	4.0	4.0	1.0	5.2	2.1
Simulated_Alloy_2	Bal.	0.5	15.0	2.0	4.0	1.0	2.7	3.3

Sample Preparation via PTA. The investigated alloys WA1 and WA1 were welded on unalloyed steel under argon atmosphere. The weld seams were 2 cm long and examined at the centre of the weld seam. The dilution between the cladding and base material was under 5 %.

Spark Spectrometry. Table 4 shows the optical emission spectrometry results. The welded alloys were named “Welded_Alloy_1” [WA1] and “Welded_Alloy_2” [WA2]. The deviation between the simulated and welded values of the single elements are within a tolerance interval of 10%. Therefore, the chemical composition of the welded alloys corresponds to the previously composition of the simulated values. The highest percentage deviations occurred for the element carbon (9.56 %). The deviations are due to the fact that the carbon values are in the range of hundred and therefore the smallest deviations of micrograms lead to the corresponding percentage deviations. The absolute deviations for carbon are a maximum of 0.06 g. Possible reasons for the lower carbon content may be due to dilution or/and alloy combustion during welding.

Table 4. Chemical composition determined by optical emission spectrometry in wt%

	C	Cr	Nb	Ni	V	Fe
Simulated_Alloy_1	0.70	14.00	4.00	4.00	1.00	Bal.
Welded_Alloy_1	0.64	14.79	4.12	4.16	1.05	-
Discrepancy (%)	9.56	5.64	2.40	3.00	5.00	-
Simulated_Alloy_2	0.50	15.00	2.00	4.00	1.00	Bal.
Welded_Alloy_2	0.48	15.62	2.03	4.16	0.98	-
Discrepancy (%)	4.00	4.13	1.50	4.00	2.00	-

Microstructure and Hardness. The carbide phase content was recalculated with JMatPro® using the composition values of WA1 and WA2 and compared with the phase contents of SA1 and SA2, as shown Fig. 5. It's evident that the newly calculated carbide content of the alloys is slightly lower from the initial calculation, as carbon has a significant influence on carbide formation [18]. Fig. 4 shows the qualitative distribution of the Elements Cr and Nb in the microstructure. Chromium is distributed over almost the entire micro-structure, especially in the eutectic areas an increased chromium concentration is visible. Furthermore, black areas can be recognised where chromium is entirely ab-sent. These areas are accordingly covered with niobium, as can be seen in the illustration. XRD measurements were conducted of SM1 to validate the previously calculated phases. The XRD result in Fig. 6 confirms the existence of the carbides $Cr_{23}C_6$, Cr_7C_3, and NbC, as well as the phases γ-Fe and α-Fe. The expression of the NbC signal is very clear, whereas the Cr23C6 is only very weakly detected due to their low content. Furthermore, the prediction of Cr7C3 carbide does not match the calculations of JMatPro®. Since these calculations are based on equilibrium conditions, the formation of carbides cannot be accurately considered due to the reaction kinetics. For a clear identification of the chromium carbides, the Fe/Cr ratio of the chromium-rich phases are required. For the M23C6 carbides, the Cr/Fe ratio is approximately 0.95, while in the M_7C_3 carbides, it ranges between 1.76 and 1.83 [19] [20]. Furthermore, vanadium carbides could not be detected, although their formation was predicted by JMatPro®. However, due to the low proportion of only 0.4 wt%, their presence could not be confirmed.

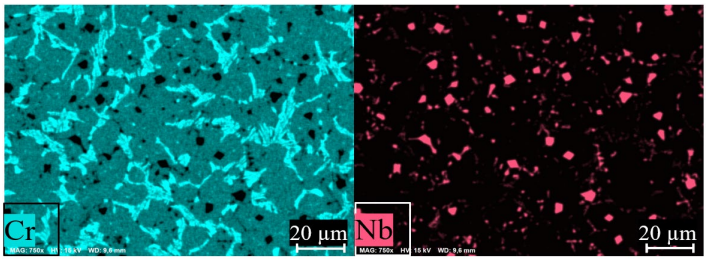

Fig. 4. EDX mapping of the elements Cr and Nb

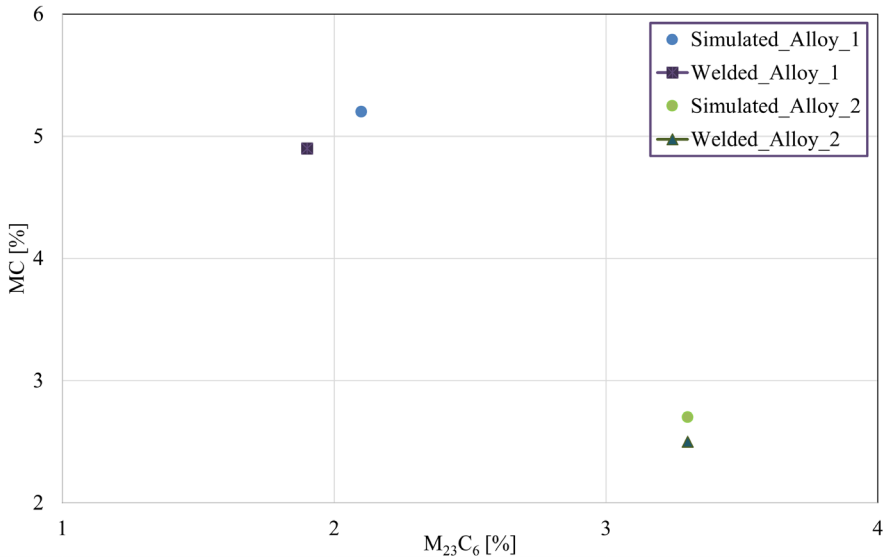

Fig. 5. Carbide content of the measured and calculated alloys

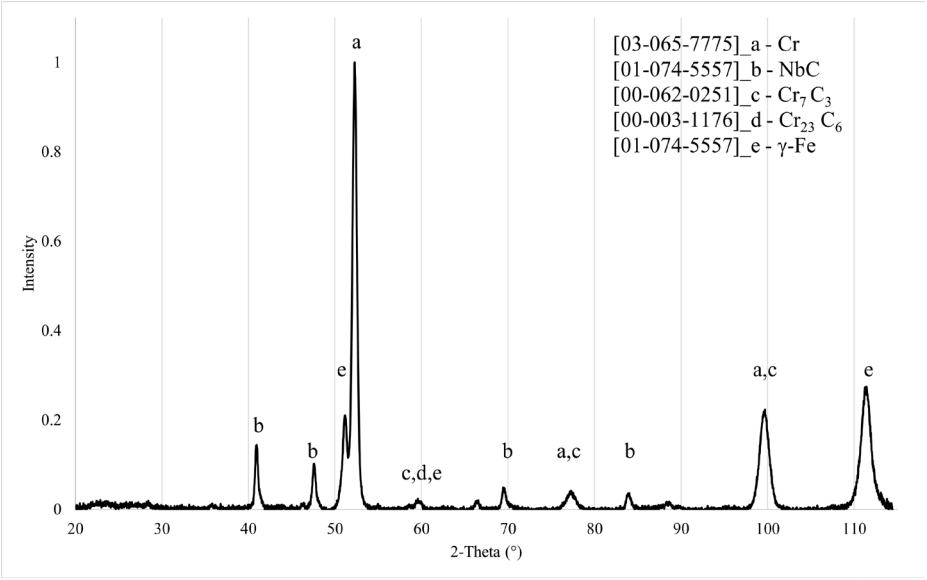

Fig. 6. XRD analysis of the WA1

Fig. 7a-b presents the microstructure of the alloys after PTA welding, with various magnifications selected (50x and 100x) to offer a comprehensive view of the micro-structural details. According to Fig. 5, WA1 has the highest amount of MC carbides with 4.9 wt%, followed by WA2 (2.5 wt%). These values correspond to the Fig. 7a-b. It can be clearly seen that in Fig. 7a the reddish MC carbides are the most recognisable in terms of size and quantity. In the other alloys, the MC carbides decrease significantly. On the other hand, the Cr23C6 / Cr7C3 content of WA1 is significantly lower (1.9 wt%). Consequently, the network-like carbide structure is much less developed compared to WA2. The matrix of both alloys consists of ferrite and austenite. It can be concluded from the microstructural images that these correspond to the simulated alloy compositions measured. The section headings are in boldface capital and lowercase letters. Second level headings are typed as part of the succeeding paragraph (like the subsection heading of this paragraph).

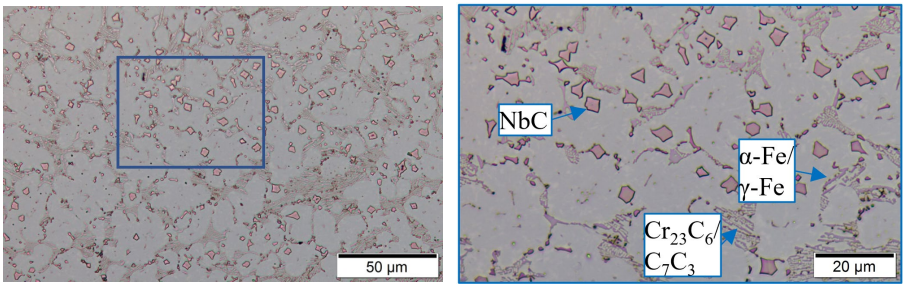

Fig. 7a. Microstructure of WA1

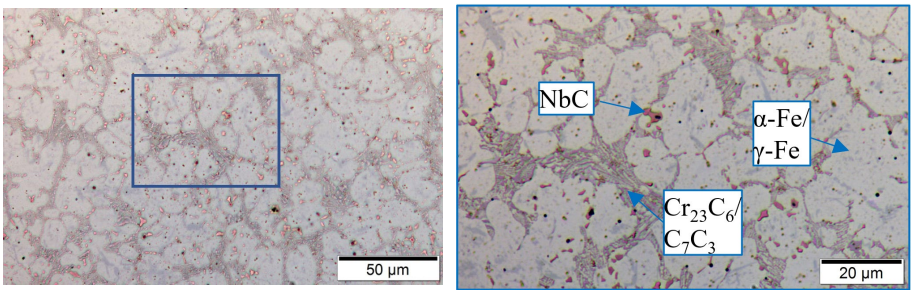

Fig. 7b. Microstructure of WA2

Fig. 8 and Fig. 9 shows the SEM images with energy-dispersive x-ray line scan measurements of the welded alloys in relation to the corresponding chromium and niobium content. The chromium contents vary according to the corresponding phase. The bright white areas represent the MC phase i.e., the niobium carbides (NbC). Accordingly, in this phase, the chromium content is lower. In WA1, with a niobium content of 4 wt%, the chromium content in these areas partially drops below 3 wt%. Due to the larger carbides in WA1, the deflections are clearer than in WA2. The shaded areas represent the M23C6 /M7C3 phase i.e., the Cr23C6/Cr7C3 carbides. According to the molecular formula, a higher chromium content is expected here. In both alloys, the chromium content increases significantly in this phase. The last phase is the ferritic/austenitic matrix, which has the highest percentage of all phases. In this phase the alloys containing at least 12 wt% chromium, which fulfil the prerequisites for corrosion resistance. This high chromium content ensures the formation of a stable and protective passive oxide layer.

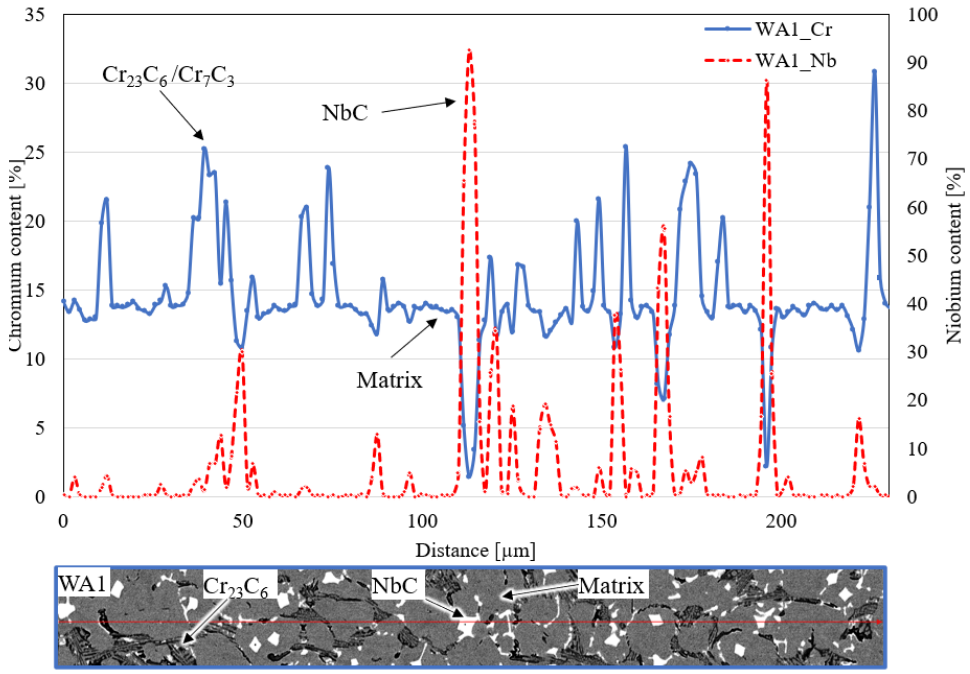

Fig. 8. SEM images with EDX line scan of WA1

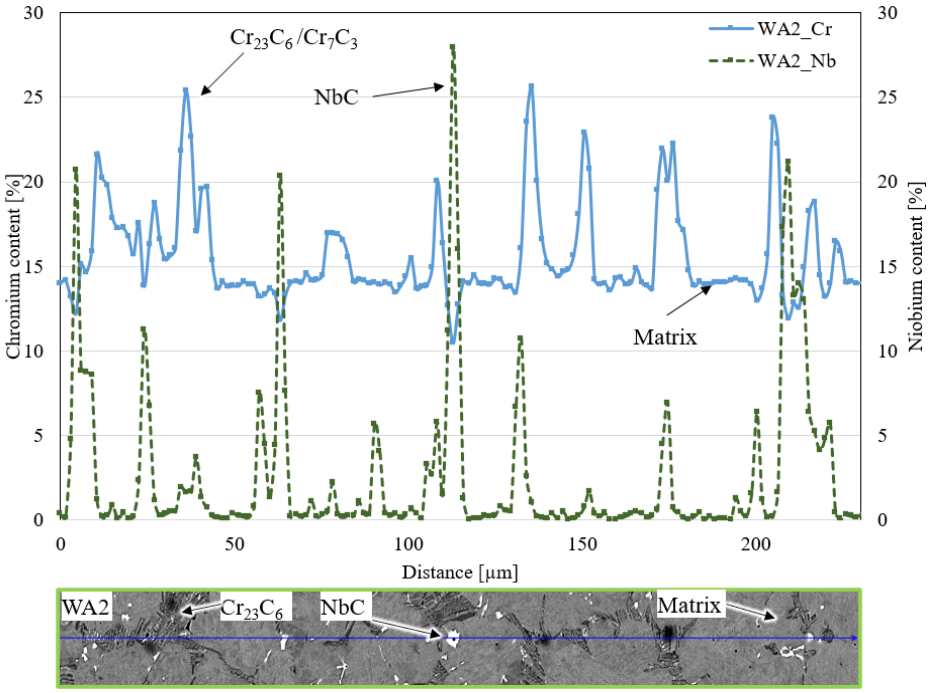

Fig. 9. SEM images with EDX line scan of WA2

Hardness measurements were carried out on both alloys after PTA, as shown in Fig. 10 . The average hardness of the WA1 is 575 HV, with minimum and maximum values of 524 and 670 HV. The WA2 alloy, on the other hand, has an average hardness of 433 HV, with minimum and maximum values of 328 and 524 HV. The higher hardness in WA1 can be attributed to its significantly higher NbC carbide content. NbC carbides can achieve a hardness of up to 2400 HV. In contrast, Cr_7C_3 /$C_{23}C_6$ carbides only achieve a hardness of up to 1500/1700 HV [21]. Furthermore, WA1 has a higher carbon content, which is favourable for the hardness formation of both the matrix and hard phases [10].

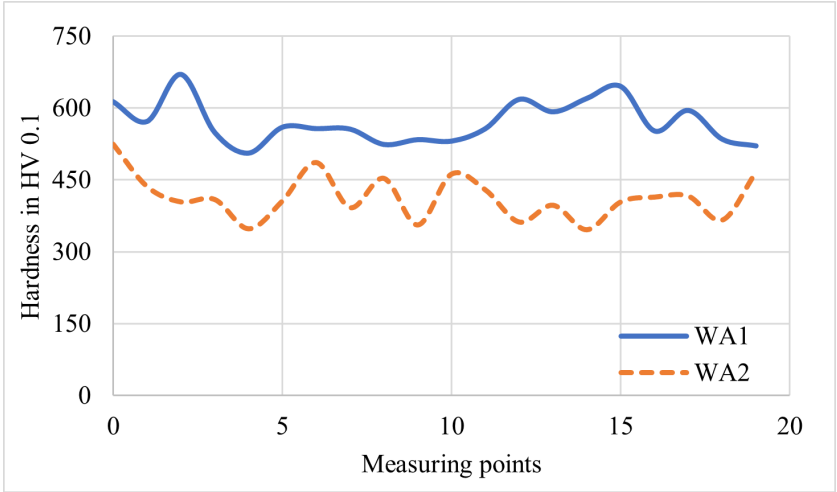

Fig. 10. Hardness measurement of the alloys WA1 and WA2

Microstructure and Hardness. In this work, a computer aided modelling method was applied to development suitable alloys for the tailored forming process chain. Initially, a design of experiments with full factorial design was formulated, by using JMatPro® and EDA®. Therefore, the elements chromium, vanadium, nickel, iron and carbon have been selected with a defined step size. The phases and temperature ranges for the calculation were also defined. After completing the calculations, 87,846 alloys were available, which were sorted according to defined requirements. These included the material properties with regard to carbides, austenite content and corrosion resistance. Regarding the carbides, it was necessary that both eutectic and carbides precipitated directly from liquid melt

were present. The MC carbides solidify directly from the melt and are characterised by high hardness, whereas the eutectic carbides dissolve during austenitisation and can thus be used for secondary hardening by heat treatment processes. With regard to formability, a high austenitisation percentage is aimed for, which extends over a long temperature interval. To ensure corrosion resistance, at least 12 wt% dissolved chromium in the matrix is required to form a passivation layer. After applying the criteria, 10 alloys were left, of which 2 were selected that had different values in terms of their different carbide phases. One alloy had a higher MC carbide content, while the other alloy had a higher eutectic carbide content. After the target alloys had been defined, they were produced by mechanical blending and welded using PTA process. The welded samples were characterised in terms of X-ray diffraction, scanning electron microscopy, spark spectrometry, hardness measurements and metallography. The optical emission spectrometry results matched predominantly to the computational results. Only the carbon content showed percentage deviations of 9.56 %, but in absolute numbers these were in the range of hundred. A recalculation of the alloys with the experimentally measured chemical composition showed minimal deviations in terms of the expected carbide contents. The metallographic images also matched the previously calculated results. A clear difference between the phases depending on the chemical composition could be determined. XRD measurements could not confirm all expected phases, such as VC, and unexpectedly confirmed the presence of Cr_7C_3, which was not predicted by JMatPro®. Energy-dispersive x-ray line scan measurements were carried out to ensure corrosion resistance. The results showed that in both alloys the chromium content in the matrix was at least 12 wt%. This chromium content ensures that a passivation layer can be generated, making the alloys corrosion-resistant. Further investigations are needed to examine in more detail the forming properties as well as the development of secondary carbides depending on the heat treatment process. The study has demonstrated that employing a computer aided modelling approach based on the CALPHAD method and materials science principles facilitates the deliberate design of target alloys, which can subsequently be fabricated through deposition welding. Therefore, the computer aided modelling approach offers the opportunity to develop alloys more precisely and efficiently according to the specific application requirements.

Acknowledgments

The results presented in this work were obtained within the Collaborative Research Centre 1153 “Process chain to produce hybrid high-performance components by Tailored Forming” in the subproject A04 (deposition welding). The authors thank the German Research Foundation (DFG) for their financial support of this project.

References

[1] N. Saunders, A.P. Miodownik, *CALPHAD: Calculation of Phase Diagrams - A Comprehensive Guide*, Bd. 1. in Pergamon Materials Series, vol. 1. Elsevier, 1998. doi: 10.1016/S1470-1804(98)X8001-6.

[2] J. Chen *u. a.*, „Design and Optimization of Heat Treatment Process Parameters for High-Molybdenum-Vanadium High-Speed Steel for Rolls“, *Materials*, Bd. 16, Nr. 22, S. 7103, Nov. 2023, doi: 10.3390/ma16227103.

[3] M. Krbata *u. a.*, „Microstructural Changes and Determination of a Continuous Cooling Transformation (CCT) Diagram Using Dilatometric Analysis of M398 High-Alloy Tool Steel Produced by Microclean Powder Metallurgy“, *Materials*, Bd. 16, Nr. 12, S. 4473, Juni 2023, doi: 10.3390/ma16124473.

[4] J. Dykas, L. Samek, A. Grajcar, und A. Kozłowska, „Modelling of Phase Diagrams and Continuous Cooling Transformation Diagrams of Medium Manganese Steels“, *Symmetry*, Bd. 15, Nr. 2, S. 381, Feb. 2023, doi: 10.3390/sym15020381.

[5] S. C. Cha *u. a.*, „CALPHAD-based alloy design for advanced automotive steels - Part I: Development of bearing steels with enhanced strength and optimized microstructure“, *Calphad*, Bd. 54, S. 165–171, 2016, doi: https://doi.org/10.1016/j.calphad.2016.04.007.

[6] A. Panda, A. K. Sahoo, R. Kumar, und R. K. Das, „A review on machinability aspects for AISI 52100 bearing steel“, *Materials Today: Proceedings*, Bd. 23, S. 617–621, 2020, doi: 10.1016/j.matpr.2019.05.422.

[7] T. Coors, Y. Faqiri, F. Saure, F. Pape, T. Hassel, und G. Poll, „Wear of Tailored Forming Steels“, *Adv Eng Mater*, S. 2201740, Mai 2023, doi: 10.1002/adem.202201740.

[8] „DIN 51819-1:2016-12, Prüfung von Schmierstoffen_- Mechanisch-dynamische Prüfung auf dem Wälzlagerschmierstoff-Prüfgerät FE8_- Teil_1: Allgemeine Arbeitsgrundlagen“, Beuth Verlag GmbH. doi: 10.31030/2577274.

[9] H. Berns, Hrsg., *Hartlegierungen und Hartverbundwerkstoffe*. Berlin, Heidelberg: Springer Berlin Heidelberg, 1998. doi: 10.1007/978-3-642-51505-7.

[10] F. Jeglitsch, „NIOBIUM IN TOOL STEELS AND CEMENTED CARBIDES“, 2002. [Online]. Verfügbar unter: https://api.semanticscholar.org/CorpusID:229360204

[11] E. Kocaman, B. Kılınç, M. Durmaz, Ş. Şen, und U. Şen, „The influence of chromium content on wear and corrosion behavior of surface alloyed steel with Fe(16−x)Crx(B,C)4 electrode“, *Engineering Science and Technology, an International Journal*, Bd. 24, Nr. 2, S. 533–542, Apr. 2021, doi: 10.1016/j.jestch.2020.08.003.

[12] S. Taylor, V. Janik, R. Grimes, und R. Dashwood, „Study on the Influence of Nickel Additions on AA7020 Formability Under Superplastic Forming Like Conditions“, *Met. Mater. Int.*, Bd. 29, Nr. 9, S. 2597–2604, Sep. 2023, doi: 10.1007/s12540-023-01396-9.

[13] T. Blohm, M. Mildebrath, M. Stonis, J. Langner, T. Hassel, und B.-A. Behrens, „Investigation of the coating thickness of plasma-transferred arc deposition welded and cross wedge rolled hybrid parts“, *Production Engineering*, Bd. 11, März 2017, doi: 10.1007/s11740-017-0734-7.

[14] J. Wilden, J. P. Bergmann, H. Frank, S. Pinzl, und F. Schreiber, „Thin Plasma- Transferred-Arc Welded Coatings - an Alternative to Thermally Sprayed Coatings?“, gehalten auf der ITSC2004, B. R. Marple und C. Moreau, Hrsg., Osaka, Japan, Mai 2004, S. 556-561. doi: 10.31399/asm.cp.itsc2004p0556.

[15] A. Y. C. Nee, Hrsg., *Handbook of Manufacturing Engineering and Technology*. London: Springer London, 2015. doi: 10.1007/978-1-4471-4670-4.

[16] U. Dilthey, Hrsg., *Schweisstechnische Fertigungsverfahren. 2: Verhalten der Werkstoffe beim Schweißen / Ulrich Dilthey*, 3., Bearb. Aufl. Berlin Heidelberg: Springer, 2005.

[17] J. Li und C. Shi, „Carbides in Special Steel“, in *Carbide in Special Steel*, in Engineering Materials. , Singapore: Springer Singapore, 2021, S. 1–57. doi: 10.1007/978-981-16-1456-9_1.

[18] L. Xu, S. Wei, J. Xing, und R. Long, „Effects of carbon content and sliding ratio on wear behavior of high-vanadium high-speed steel (HVHSS) under high-stress rolling–sliding contact“, *Tribology International*, Bd. 70, S. 34–41, Feb. 2014, doi: 10.1016/j.triboint.2013.09.021.

[19] K. Wieczerzak, P. Bała, M. Stępień, G. Cios, und T. Kozieł, „The Characterization Of Cast Fe-Cr-C Alloy“, *Archives of Metallurgy and Materials*, Bd. 60, Nr. 2, S. 779–782, Juni 2015, doi: 10.1515/amm-2015-0206.

[20] J.-H. Chen *u. a.*, „Microstructure and abrasive wear properties of Fe-Cr-C hardfacing alloy cladding manufactured by Gas Tungsten Arc Welding (GTAW)“, *Met. Mater. Int.*, Bd. 19, Nr. 1, S. 93–98, Jän. 2013, doi: 10.1007/s12540-013-1015-4.

[21] H. Berns, „Entstehung des Gefüges bei der Fertigung“, in *Hartlegierungen und Hartverbundwerkstoffe*, H. Berns, Hrsg., Berlin, Heidelberg: Springer Berlin Heidelberg, 1998, S. 13–25. doi: 10.1007/978-3-642-51505-7_2.

The publication of this article was funded by the Leibniz University Hannover (TIB) LUH